Optometry & Contact Lenses · Vol. 4, No. 8, pp. 272-280, 2024
https://doi.org/10.54352/dozv.TSGX1738
Published online in English as Open Access: 27.09.2024

A Review on current developments in early ectasia detection – the corneal biomechanical analysis

Robert Herber[1,3], Frederik Raiskup[2,3]

[1] Ph.D., M.Sc • [2] Prof., Ph.D., Dr.Sc. • [3] Department of Ophthalmology, University Hospital Carl Gustav Carus, Dresden University of Technology, Dresden, Germany

Received 4 June 2024; accepted 10 July 2024

Abstract

Purpose. Topographic and tomographic parameters are often not sufficient for early diagnosis of corneal changes. Pathological processes begin in the microstructure before topographic/tomographic abnormalities become apparent. Biomechanical parameters correlate strongly with microscopic structural parameters, while they can be used for early detection of ectasia.

Material and Methods. This review summarizes the biomechanical properties of the cornea with regard to the detection of early ectasia and keratoconus. Air-puff tonometry is used to record the deformation behavior of the cornea and to derive corneal deformation parameters and biomechanical indices for ectasia detection.

Results. The biomechanical parameters in keratoconus differ significantly from those of healthy eyes. Changes in the cornea can be detected even before topographic or tomographic changes. Artificial intelligence approaches support the merging of the numerous available data on single parameters for appropriate handling in clinical practice.

Conclusion. Examination of corneal biomechanics using air-puff tonometry is a new method to detect possible early changes in the tissue. The biomechanical parameters, especially those of Scheimpflug-based air-puff tonometry, reveal changes before they are visible on topography or tomography. This is of great importance in refractive surgery, but also in the management of keratoconus.

Keywords

Corneal biomechanics, keratoconus, early ectasia, air-puff tonometry, Scheimpflug imaging

Introduction

Ectatic corneal disease is characterized by an irregular change in the anterior and posterior surface of the cornea and an abnormal distribution of corneal thickness, which can lead to a significant reduction in visual acuity. The best-known forms include keratoconus and pellucid marginal degeneration (PMD).[1] Another form of corneal ectasia is iatrogenically induced ectasia following laser refractive surgery (post laser vision correction ectasia, post LVC ectasia).[2] The incidence of post LVC ectasia is between 0.04 % and 0.6 %.[3,4] According to Randleman et al., the risk factors for post LVC ectasia include thick corneal flap (in laser in situ keratomileusis), high ablation depth (equivalent to residual stromal thickness (RSD)), young patient age, thin cornea, and higher myopia, but the presence of early or undetected keratoconus.[5,6] Even the modern SMILE procedure (Small-Incision Lenticule Extraction) does not prevent post LVC ectasia, especially if corneas with borderline or suspected ectasia are treated.[4,7] This rare but serious complication can occur initially or after several months to years and can permanently reduce the patient's quality of vision. Reliable preoperative diagnostics are essential to prevent this. Particular attention is paid to screening methods that enable early detection of corneal ectasia. However, it is also important to detect the progression of the disease at a very early stage, to prevent vision loss when the ectasia manifests as keratoconus, and to allow treatments to restore corneal stability, such as corneal cross-linking.[8] If the disease is not yet advanced, corneal reshaping of the keratoconic cornea can also be performed in combination with an excimer laser.[9]

Currently, the most commonly used diagnostic tools measure geometric (static) properties of the cornea, such as corneal thickness, curvature, and optical aberrations. However, these methods do not reflect changes under stress. The behavior of the cornea under stress (dynamic characterization) is determined by the biomechanical properties of the cornea. Macroscopic biomechanical properties such as elasticity, stiffness, viscosity, shear behavior, etc. are determined by the microscopic structure (arrangement of collagen lamellae, chemical composition, etc.).

Pathological changes first occur in the microstructure before macroscopic abnormalities can be detected. Such microscopic changes have been clearly demonstrated in tissue samples. Hayes et al. demonstrated a loss and altered orientation of collagen fibrils within the corneal stroma, which was associated with typical changes in corneal curvature and thickness.[10] In clinical practice, a fast, non-invasive and non-contact method is needed to measure corneal properties related to the microstructure of the cornea. Therefore, air-puff tonometry has been introduced to measure biomechanical parameters of the cornea that meet these requirements and provide information about the microstructure and, in particular, structural abnormalities. This review summarizes the use of biomechanical measurements of the cornea for the detection of ectasia, especially keratoconus.

Basics in corneal biomechanics

The corneal stroma, which makes up 90 % of the corneal thickness, determines the biomechanical properties of the cornea. It is a tissue with an extraordinary shape, a certain stability and a high degree of optical transparency.[11] The entire cornea is subject to internal tension from intraocular pressure (IOP) and external tension from the eyelids, extraocular muscles, and the effects of eye rubbing. Mechanical stability against the aforementioned external influences and optical transparency are mainly achieved by the fibrils of the corneal tissue. The so-called microfibrils are interweaved like a rope and form a fibril. This gives the structure high mechanical strength. The diameter of the individual fibrils and the distance between them is constant in the central area of the cornea and in the depth of the stroma. Towards the limbus, the diameter and spacing of the fibrils increase, which is associated with increased corneal thickness in the limbal area and different biomechanical properties between the central and peripheral cornea.[12] The overlying structure of the collagen fibrils is formed by the lamellae. These run parallel to the surface and are stacked on top of each other. The collagen fibrils are embedded in a viscous matrix consisting mainly of proteoglycans (PG), glycosaminoglycans (GAG), and keratocytes.[13] In the anterior stroma, the horizontal and vertical interweaving of collagen is denser than in the posterior region. As a result, the stiffness in the anterior stroma is also higher than in the posterior.[14] Overall, the cornea can be described as having a

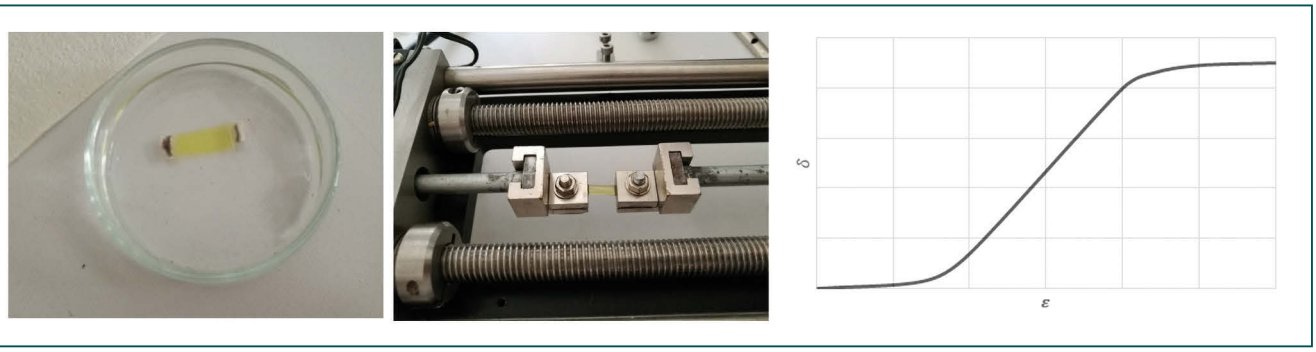

Figure 1: Preparation of the corneal sample (strip, left) for an uniaxial stress-strain measurement (center) resulting in a typical non-linear stress-strain curve (right). σ = stress, ε = strain.

heterogeneous, nonlinear elastic, anisotropic, and viscoelastic mechanical behavior due to the composition of the collagen fibrils, the organization and interaction between the fibrils, and the viscous matrix of PG and GAG.[15]

Corneal biomechanics in vivo

To determine the biomechanical behavior of the cornea, a defined force must be applied to the tissue to deform it. In the past, this could only be done ex vivo in the laboratory using stress-strain measurements (**Figure 1**).[16]

Two devices are available for in vivo investigation of corneal biomechanics: the Ocular Response Analyzer (ORA, Reichert Technology, Buffalo, New York, USA)[17] and the Dynamic Scheimpflug Analyzer (Corvis ST, Oculus Optikgeraete GmbH, Wetzlar, Deutschland).[18] Both devices use an air puff to deform the cornea. The devices differ in the technology used to record the deformation and in the display of the so-called deformation parameters or biomechanically related parameters. With ORA, corneal deformation is measured using an infrared light beam that is reflected during the first applanation (inward movement) and during the second applanation (outward movement) of the cornea and detected by a sensor. The parameters of the measurement are the corneal hysteresis (CH), which describes the viscous damping of the corneal tissue, and the corneal resistance factor (CRF), which represents the overall resistance to corneal deformation.[19] It should be noted that these two parameters are not the same as stiffness, since stiffness is a measure of elasticity, while CH or CRF is a measure of viscoelasticity.[20] A representative measurement result of the ORA is shown in Figure [2].

The Corvis ST (Corneal Visualization Scheimpflug Technology) records the deformation of the cornea induced by the air pulse using the Scheimpflug principle. An ultra-high-speed camera (4,300 frames/sec) generates 140 individual images within 31 ms of the onset of the air pulse. The phases of corneal deformation are shown in **Figure 3**. The measurement is performed in the horizontal plane only and their output the so-called dynamic corneal response (DCR) parameters (**Table 1**)

When measuring with the ORA or Corvis ST, the cornea cannot be considered in an isolated environment, such as in a stress-strain measurement. The cornea is part of the eye and the intraocular pressure (IOP) acts within the cornea. In addition, corneal thickness varies from individual to individual, and corneal structure changes with age. These factors influence the deformation behavior of the cornea and must be taken into account and corrected for when determining the biomechanical parameters, as proposed for the ORA in 2015.[21]

The IOP has the strongest influence on the deformation behavior, i. e. the higher the IOP, the lower the deformation of the cornea after the application of the air pulse. This affects

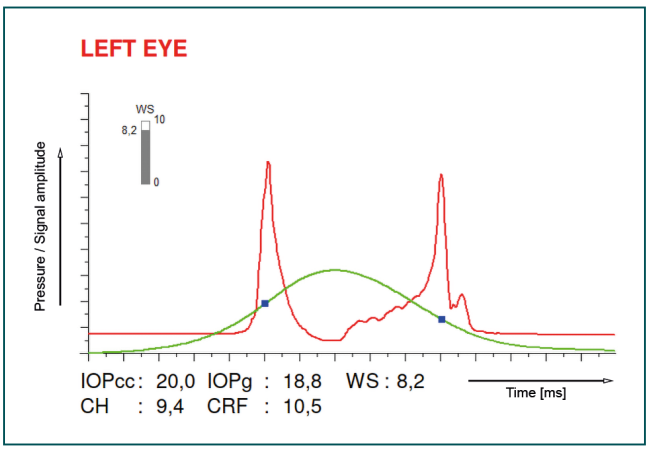

Figure 2: Measurement result of the Ocular Response Analyzer providing intraocular pressure values (IOPg), corrected intraocular pressure values (IOPcc), corneal hysteresis (CH), corneal resistance factor (CRF), and wavescore (WS, reliability of the signals). Green curve represents the pressure signal of the air-puff. The red curve represents the applanation signal of the cornea.

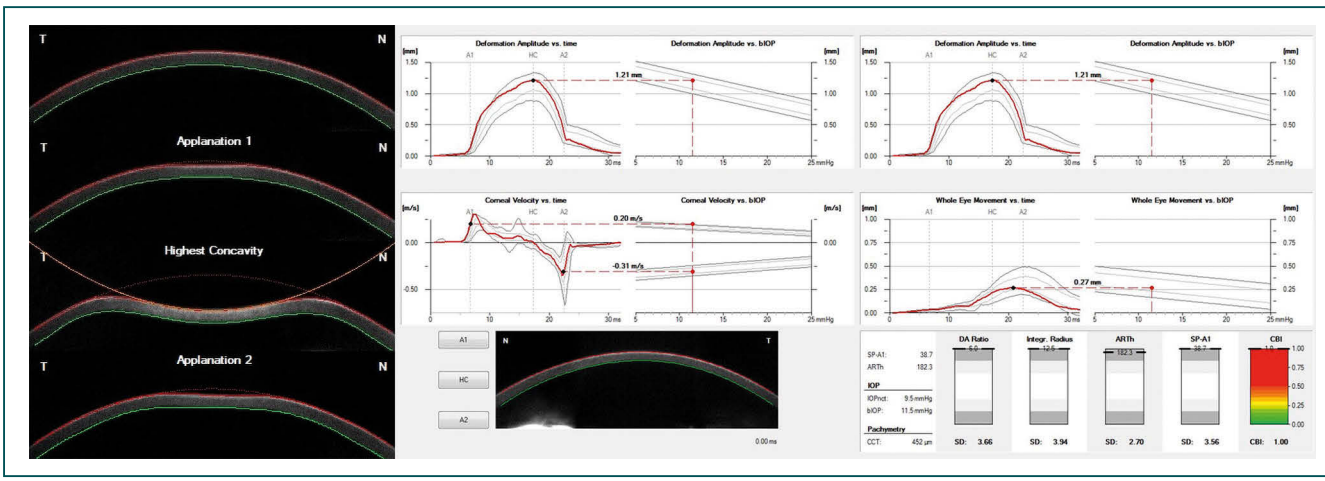

Figure 3: Scheimpflug images of the Corvis ST measurement (left). Upper left to downwards: initial state, first applanation, state of highest concavity, and second applanation. Right: measurement results with the clinical important parameters: stiffness parameter at first applanation (SPA1), intraocular pressure (IOPnct), biomechanical corrected intraocular pressure (bIOP), central corneal thickness (CCT), deformation amplitude ratio (DA ratio), integrated inverse radius (Integr. Radius), and Corvis Biomechanical Index (CBI).

Table 1: Overview of the clinically relevant parameters from ORA (corneal hysteresis, corneal resistance factor) and Corvis ST (integrated inverse radius, stiffness parameter at 1st applanation and Corvis Biomechanical Index).

Parameter	Description
CH	Corneal hysteresis [mmHg]
CRF	Corneal resistance factor [mmHg]
IIR	Integrated inverse radius (sum of inverse (concave) radius between 1st and 2nd applanation [mm^{-1}]
SPA1	Stiffness parameter at 1st applanation [mmHg/mm]
CBI	Corvis Biomechanical Index

the deformation parameters of both devices, e. g. there is a negative correlation between CH and IOP (ORA) and a positive correlation between the stiffness parameter of the first applanation (SPA1) and IOP (Corvis ST) in healthy eyes.[22] The thickness of the cornea also influences the deformation behavior, as greater corneal thickness provides greater resistance to deformation (positive association between CH and SPA1 with corneal thickness) in healthy eyes.[22] The structure of the cornea changes with age. However, these changes should not be considered pathological, but rather age-related.[23]

Detection of keratoconus using corneal biomechanics

As previously mentioned, corneal ectasia, specifically keratoconus is a disease of the cornea characterized primarily by a steepening of the corneal curvature and a thinning of the stromal tissue. These changes are the result of a biomechanical weakening of the tissue and consequently these corneas exhibit reduced biomechanical rigidity.[24,25,26] KC eyes have lower CRF and CH values than healthy eyes (**Figure 4**).[27,28,29] The reason for this is the lower resistance of the cornea to the air puff, partly due to the reduced corneal thickness. Despite the same viscosity of the ground substance, the CH (simplified: difference of P1 – P2) is reduced because the first applanation is reached faster and the back movement is delayed.[19]

Figure 4 shows the significant difference between healthy and keratoconic eyes. There is little overlap between the groups, indicating good diagnostic discriminative power, with a sensitivity and specificity of 87 % for CH and 80 % for CRF at a cut-off of 9.4 and 8.65, respectively.[22]

Regarding the DCR parameters, it was shown that keratoconus corneas have a lower resistance to the air puff and therefore a lower stiffness. This was expressed by the fact that the IIR parameter showed higher values in the keratoconus group compared to healthy subjects, indicating a more deformable behavior or a lower resistance to the applied force (**Figure 5**).[22] The SPA1 parameter had lower values indicating also a lower stiffness of the cornea (**Figure 5**).[22,30,31]

Figure 5 shows the distribution of IIR and SPA1 values for healthy and keratoconus eyes in the box plot. It showed a good discriminatory power for both parameters between the

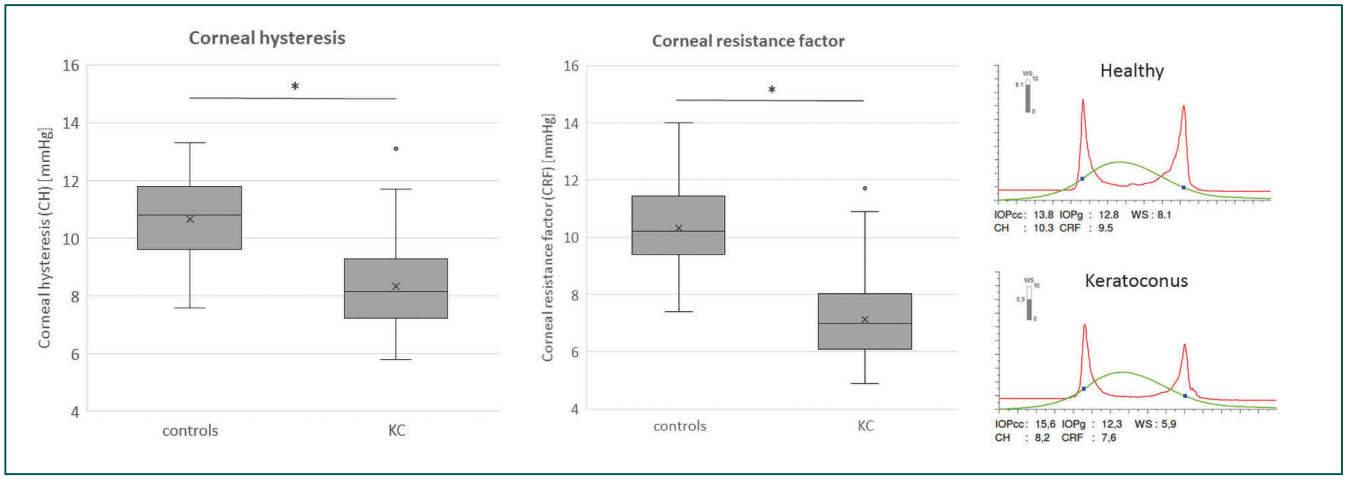

Figure 4: Graphical interpretation (Box-plot, cross represents mean value) of the study results published by Herber et al. between healthy eyes (controls) and keratoconic eyes (KC).[22] Corneal hysteresis (CH) and corneal resistance factor (CRF) were statistically significantly lower in KC compared to controls (P-value < 0.05 is considered as statistical significance (*)). Right: Representative measurements result of a healthy and keratoconic eye.

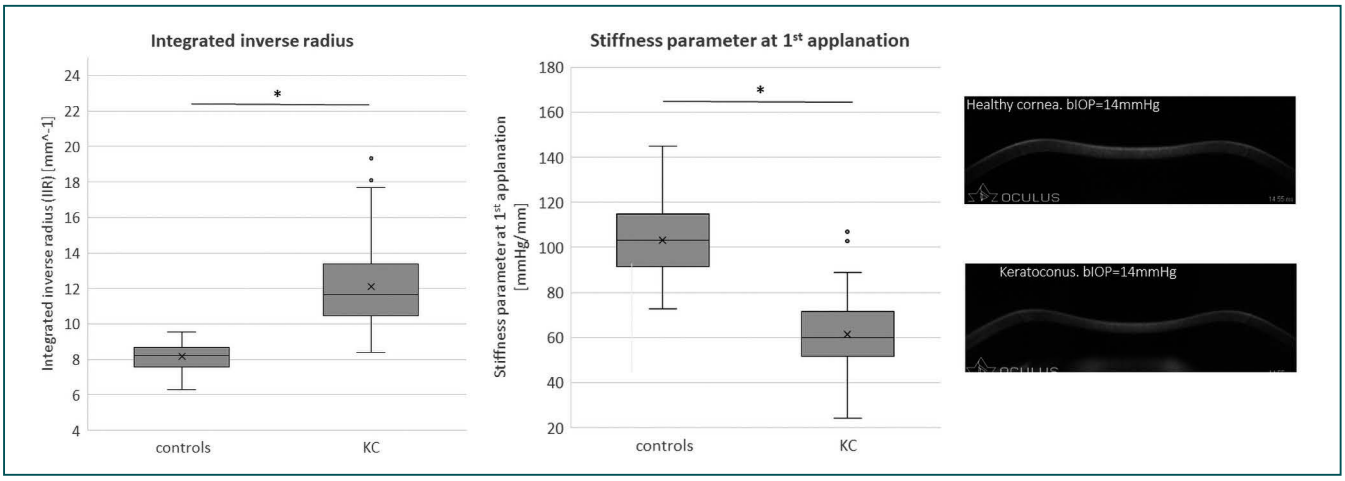

Figure 5: Graphical interpretation (Box-plot, cross represents mean value) of the study results published by Herber et al. between healthy eyes (controls) and keratoconic eyes (KC).[22] Integrated inverse radius (IIR) and stiffness parameter at 1st applanation (SPA1) were statistically significantly higher and lower in KC compared to controls, respectively (P-value < 0.05 is considered as statistical significance (*)). Right: Scheimpflug image of a healthy eye and a keratoconic eye with equal IOP and same measurement point. The KC eye demonstrated a more deformable cornea.

study cohorts. The sensitivity and specificity for IIR were 90 % and 93 %, respectively, which was statistically significantly better than for CH and CRF. The SPA1 parameter achieved a sensitivity and specificity of 85 % and 90 % respectively, comparable to CRF but statistically significantly better than CH.[22]

Due to the large number of DCR parameters generated by the Corvis ST, a quick overview and assessment of the risk of ectasia is limited. For this reason, the Corvis Biomechanical Index (CBI) was developed to achieve a high degree of discrimination between healthy and keratoconus eyes from a linear combination of different DCR parameters and, most importantly, to present them graphically so that the clinician can make a quick assessment.[32] As shown in **Figure 3**, the CBI has values between 0 ("healthy") and 1 ("pathological") (lower right). These are supported by a color scale (green corresponds to "healthy" and red corresponds to "pathological"). In the pilot study by Vinciguerra et al. a sensitivity and specificity of 94 % and 100 % were achieved in the training data set and 98 % and 100 % in the validation data set with a cut-off of 0.5.[32] Similar results were shown by Sedaghat et al. and were also achieved in the study by Herber et al.[22,31] Compared to the other parameters of the Corvis ST, but also to the ORA, the CBI showed the highest sensitivity (97 %) and specificity (98 %) for discriminating between healthy and keratoconic eyes.[22]

Since these studies compared clinical keratoconus eyes with healthy eyes, the question of clinical relevance arises when topography or tomography systems are available in clinical practice. As described above, it is assumed that the biomechanical changes occur before the topographic and tomographic changes, thus providing a clinical relevance for biomechanical measurement in early keratoconus, which is described in the following section.

Detection of early ectasia using corneal biomechanics

To test whether new diagnostic methods are relevant for the detection of early ectasia, the following assumption is necessary, based on the Global Consensus on Keratoconus and Ectatic Disease, which assumes that keratoconus is an asymmetric but bilateral disease.[1] In some keratoconus patients, the asymmetry is so pronounced that these patients have clinical keratoconus in one eye (very asymmetric ectasia-ectasia eye, VAE-E) but "normal" topography and/or even "normal" tomography in the other eye (very asymmetric ectasia - normal topography and/or tomography, VAE-NT/NTT). Previous studies have shown that clinical keratoconus develops from a normal eye in 15 to 35 percent of cases.[33,34] Therefore, those cases could be assumed as very early or suspicious ectatic corneas and represent an appropriate study cohort to evaluate the diagnostic ability of novel technologies or indices.

This requires an objective definition of "normal" topography. The following definitions have been used in recent years: maximum keratometry value (K_{max}) < 47.0 D, inferior-superior difference of keratometry values < 1.45 D, and KISA% < 60.[35,36] A Belin-Ambrosio total deviation (BAD D, from the Pentacam) of less than 1.6 provides reliable information for defining a tomographically "normal" cornea.

In a previous study, normal corneas were compared with VAE-NT, VAE-NTT, VAE-E, mild, and moderate KC regarding corneal biomechanical parameters of ORA and Corvis ST.[36] In the baseline demographics, no difference in IOP and thinnest corneal thickness was found between normal corneas and VAE-NTT cases, indicating that both cohorts were matched with respect to inclusion criteria and influencing factors (age, corneal thickness, and IOP) of corneal biomechanical parameters. All other groups were matched regarding IOP and age.[36]

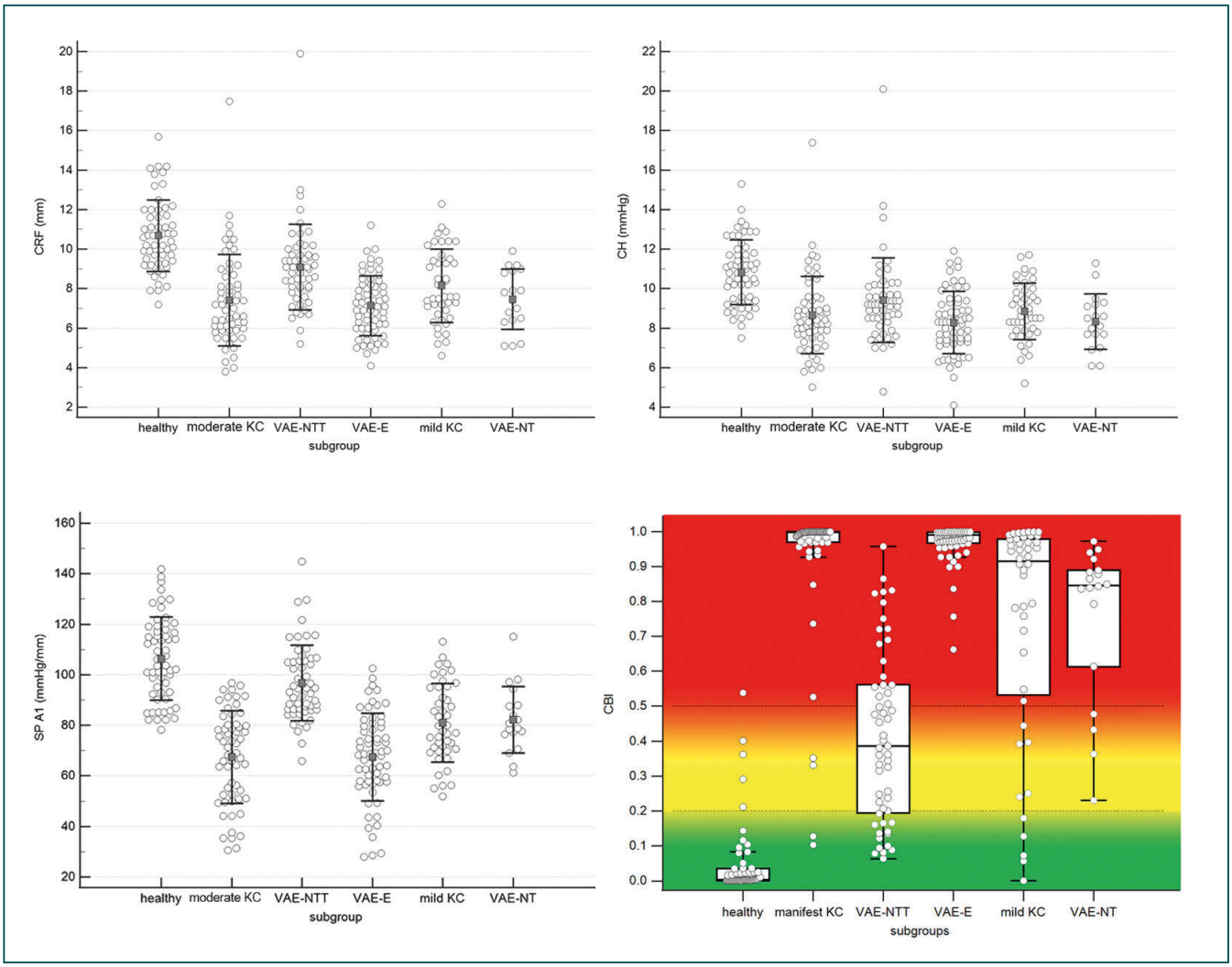

Figure 6: Comparison of Ocular Response Analyzer parameters (CRF and CH) and dynamic corneal response parameters (SPA1 and CBI) between the different subgroups using dot plots.[36] Mean and standard deviation are marked as square and lines. CBI = Corvis Biomechanical Index; CRF = corneal resistance factor; CH = corneal hysteresis; E = ectasia; KC = keratoconus; NT = normal topography; NTT = normal topography and tomography; PA1 = stiffness parameter at 1st applanation; VAE = very asymmetric ectasia.

The results showed that CH, CRF, SPA1, and CBI were the only four parameters that were statistically significantly different between normal corneas and all ectasia subgroups (VAE-NTT, VAE-NT, mild KC, moderate KC, and VAE-E). The distribution of the collected data is shown in **Figure 6**. Despite the statistical significance between healthy eyes and all subgroups of ectasia, the plots of CH, CRF and SPA1 show a non-negligible overlap between the groups. A better discrimination between groups was found for CBI, where the healthy eyes were between 0.0 and 0.2, the VAE-NTT cases between 0.2 and 0.5, and all other groups (mild, moderate KC, VAE-Nt and VAE-E) between 0.5 and 1.0. This resulted in a high discriminatory power of the CBI to distinguish normal eyes from VAE-NTT cases with a sensitivity and specificity of 70.9 % and 93.1 %, respectively, and normal eyes from all ectatic subgroups with a sensitivity and specificity of 90.3 % and 93.1 %, respectively. Compared to CH, CRF and SPA1, these CBI results were statistically significant.[36] Another parameter for the detection of KC was also available in the first generation of the ORA and was called "keratoconus score" or "keratoconus match index" (KMI).[37] The measured KMI value was compared to an existing normative database, including other specific parameters of the ORA. Studies showed that the KMI had a higher sensitivity in KC detection than the CH, but was comparable to the CRF.[22,31] However, in another study, KMI was not statistically significantly different between healthy subjects and VAE-NTT, and VAE-NT, resulting in less clinically useful diagnostic ability for early detection of KC.[36]

Previous studies have shown that CH and CRF were unable to discriminate normal eyes from early or mild KC when corneal thickness was matched between groups, with sensitivity and specificity ranging from 68 % to 87 % and 63 % to 79 %, respectively.[38,39]

However, other studies have shown controversial results for CBI in the early detection of keratoconus. A Japanese study found a sensitivity and specificity of 30 % and 99 %, respectively.[40] A study by Steinberg et al. using similar inclusion and exclusion criteria also found a sensitivity and specificity

of 67 %.[41] However, it should be noted that the eyes (healthy and VAE-NT/NTT) in such studies are absolutely equivalent with respect to objective criteria (topography and tomography) and that the dynamic measurement provides additional information and a possible indication of the presence of ectasia. A definitive diagnosis based on biomechanics alone is not possible due to the influencing factors described above, as these cannot be sufficiently corrected and standardized. Therefore, real-world data may differ from the study data reported here.

Combination of corneal biomechanics and corneal tomography

The development of computer technology has had a major impact on the technical development of medical diagnostic devices. This has also led to the development of artificial intelligence (AI), which means, for example, that a machine can be taught a process so precisely that it can reproduce it.[42] The huge amount of data provided by new types of measurement devices, as shown above for the Corvis ST, makes the interpretation of clinical results increasingly complex for the individual user. Therefore, machine learning (ML), which is part of AI, helps to solve this problem. A common application is supervised learning, which uses a data set to predict a target feature (e. g., "healthy" or "pathological") based on certain independent features.[42] There are several algorithms for solving classification problems, such as linear or logistic regression, decision trees, or random forests.[42]

Since the Pentacam and Corvis ST are manufactured and sold by Oculus (Wetzlar, Germany) and both devices write to the same patient database, both biomechanical and tomographic data are available to the software. Ambrosio et al. were the first to investigate the approach of combining biomechanical data with tomographic data using artificial intelligence algorithms. In their pilot study, different approaches were tested to determine which of the algorithms (random forest, linear regression analysis, and support vector machine) provided the best discrimination between healthy eyes and different stages of ectasia (VAE-NT, clinical CK). The random forest algorithm proved to be particularly effective and led to the clinical parameter "Tomographic Biomechanical Index". It detected both clinical KC with 100 % and early ectasia with sensitivity and specificity of 90 % and 96 %, respectively.[35] Subsequently, other studies from different countries (other ethnic groups) were not able to confirm the high accuracy of the TBI,[40,41,43,44] which led to an optimization process with a much larger data set.[45] However, this new approach needs to be validated in future studies.

Conclusion

Examination of corneal biomechanics using air-puff tonometry is a new method to detect possible early changes in the tissue. The biomechanical parameters, especially those of Scheimpflug-based air-puff tonometry, reveal changes before they are visible on topography or tomography. This is of great importance in refractive surgery, but also in the management of keratoconus.

Financial disclosure

This article did not receive any specific grant from funding agencies in the public, commercial, or not-for-profit sectors.

Corresponding author

Dr. Robert Herber

E-Mail:
robert.herber@ukdd.de

References

1 Gomes, J. A. P., Tan, D., Rapuano, C. J., Belin , M. W., Ambrosio, R., Guell, J. L., Malecaze, F., Nishida, K., Sangwan, V. S. (2015). Global consensus on keratoconus and ectatic diseases. Cornea, 34, 359–369.

2 Seiler, T., Quurke, A. W. (1998). Iatrogenic keratectasia after LASIK in a case of forme fruste keratoconus. J. Cataract Refract. Surg., 1007-1009.

3 Wolle, M. A., Randleman, J. B., Woodward, M. A. (2016). Complications of Refractive Surgery: Ectasia After Refractive Surgery. Int. Ophthalmol. Clin., 56, 127-139.

4 Brar, S., Roopashree, C. R., Ganesh, S. (2021). Incidence of Ectasia After SMILE From a High-Volume Refractive Surgery Center in India. J. Refract. Surg., 37, 800-808.

5 Randleman, J. B., Woodward, M., Lynn, M. J., Stulting, R. D. (2008). Risk assessment for ectasia after corneal refractive surgery. Ophthalmology, 115, 37-50.

6 Moshirfar, M., Tukan, A. N., Bundogji, N., Liu, H. Y., McCabe, S. E., Ronquillo, Y. C., Hoopes, P. C. (2021). Ectasia After Corneal Refractive Surgery: A Systematic Review. Ophthalmol .Ther., 10, 753-776.

7 Moshirfar, M., Albarracin, J. C., Desautels, J. D., Birdsong, O. C., Linn, S. H., Hoopes, P. C. Sr. (2017). Ectasia following small-incision lenticule extraction (SMILE): a review of the literature. Clin. Ophthalmol., 11, 1683-1688.

8 Raiskup, F., Herber, R., Lenk, J., Pillunat, L. E., Spoerl, E. (2024). Cross-linking with UV-A and riboflavin in progressive keratoconus: From laboratory to clinical practice - developments over 25 years. Prog. Retin. Eye Res., 102, 101276.

9 Herber, R., Raiskup, F. (2024) Neue Entwicklungen in der Hornhautvernetzung zur Behandlung von Keratokonus mit dem Ziel die Hornhautform zu regularisieren. Optom. Contact Lenses, 4, 72-81.

10 Hayes, S., Boote, C, Tuft, S. J., Quantock, A. J., Meek, K. M. (2007). A study of corneal thickness, shape and collagen .organisation in keratoconus using videokeratography and X-ray scattering techniques. Exp. Eye Res., 84, 423-434.

11 Meek, K. M., Knupp, C. (2015). Corneal structure and transparency. Prog. Retin. Eye Res. 49, 1-16.

12 Roberts, C. J., Dupps, W. J, Jr., Downs, J. C. (2018). Biomechanics of the Eye. Kugler Publications, Amsterdam, Netherlands.

13 Ambrosio, R, Jr. (2016). Corneal biomechanics: From theory to practice. Kugler Publications, Amsterdam, Netherlands.

14 Randleman, J. B., Dawson, D. G., Grossniklaus, H. E., McCarey, B. E., Edelhauser, H. F. (2008). Depth-dependent cohesive tensile strength in human donor corneas: implications for refractive surgery. J. Refract. Surg., 24, S85-89.

15 Kling, S., Hafezi, F. (2017). Corneal biomechanics - a review. Ophthalmic Physiol. Opt., 37, 240-252.

16 Wollensak, G., Spoerl, E., Seiler, T. (2003). Stress-strain measurements of human and porcine corneas after riboflavin-ultraviolet-A-induced cross-linking. J. Cataract Refract. Surg., 29, 1780-1785.

17 Luce, D. A. (2005). Determining in vivo biomechanical properties of the cornea with an ocular response analyzer. J. Cataract Refract. Surg., 31, 156-162.

18 Hon, Y., Lam, A. K. (2013). Corneal deformation measurement using Scheimpflug noncontact tonometry. Optom. Vis. Sci., 90, e1-8.

19 Sporl, E., Terai, N., Haustein, M., Bohm, A. G., Raiskup-Wolf, F., Pillunat, L. E. (2009). [Biomechanical condition of the cornea as a new indicator for pathological and structural changes]. Ophthalmologe, 106, 512-520.

20 Roberts, C. J. (2014). Concepts and misconceptions in corneal biomechanics. J. Cataract Refract. Surg., 40, 862-869.

21 Spoerl, E., Pillunat, K. R., Kuhlisch, E., Pillunat, L. E. (2015). Concept for analyzing biomechanical parameters in clinical studies. Cont. Lens Anterior Eye.

22 Herber, R., Ramm, L., Spoerl, E., Raiskup, F., Pillunat, L. E., Terai, N (2019). Assessment of corneal biomechanical parameters in healthy and keratoconic eyes using dynamic bidirectional applanation device and dynamic Scheimpflug analyzer. J. Cataract Refract. Surg., 45, 778-788.

23 Herber, R., Kaiser, A., Grahlert, X., Range, U., Raiskup, F., Pillunat, L. E., Sporl, E. (2020). [Statistical analysis of correlated measurement data in ophthalmology : Tutorial for the application of the linear mixed model in SPSS and R using corneal biomechanical parameters]. Ophthalmologe, 117, 27-35.

24 Roberts, C. J., Dupps, W. J, Jr. (2014). Biomechanics of corneal ectasia and biomechanical treatments. J. Cataract Refract. Surg., 40, 991-998.

25 Andreassen, T. T., Simonsen, A. H., Oxlund, H. (1980). Biomechanical properties of keratoconus and normal corneas. Exp. Eye Res., 31, 435-441.

26 Lohmuller, R., Bohringer, D., Maier, P. C., Ross, A. K., Schlunck, G., Reinhard, T., Lang, S. J. (2023). [Keratoconus: biomechanics ex vivo]. Klin. Monbl. Augenheilkd., 240, 774-778.

27 Galletti, J. G., Pförtner, T., Bonthoux, F. F. (2012). Improved keratoconus detection by ocular response analyzer testing after consideration of corneal thickness as a confounding factor. J. Refract. Surg., 3, 202–208.

28 Piñero, D. P., Alio, J. L., Barraquer, R. I., Michael, R., Jiménez, R. (2010). Corneal biomechanics, refraction, and corneal aberrometry in keratoconus: An integrated study. Invest. Ophthalmol. Vis. Sci., 51, 1948–1955.

29 Touboul, D., Benard, A., Mahmoud, A. M., Gallois, A., Colin, J., Roberts, C. J. (2011). Early biomechanical keratoconus pattern measured with an ocular response analyzer: curve analysis. J. Cataract Refract. Surg., 37, 2144–2150.

30 Roberts, C. J., Mahmoud, A. M., Bons, J. P., Hossain, A., Elsheikh, A., Vinciguerra, R., Vinciguerra, P., Ambrosio, R. Jr. (2017). Introduction of Two Novel Stiffness Parameters and Interpretation of Air Puff-Induced Biomechanical Deformation Parameters With a Dynamic Scheimpflug Analyzer. J. Refract. Surg., 33, 266-273.

31 Sedaghat, M.-R., Momeni-Moghaddam, H., Ambrósio, R., Heidari, H.-R., Maddah, N., Danesh, Z., Sabzi, F. (2018). Diagnostic Ability of Corneal Shape and Biomechanical Parameters for Detecting Frank Keratoconus. Cornea 37, 1025-1034.

32 Vinciguerra, R., Ambrosio, R., Jr., Elsheikh, A., Roberts, C. J., Lopes, B., Morenghi, E., Azzolini, C., Vinciguerra, P. (2016). Detection of Keratoconus With a New Biomechanical Index. J. Refract. Surg., 32, 803-810.

33 Shirayama-Suzuki ,M., Amano, S., Honda, N., Usui, T., Yamagami, S., Oshika, T. (2009). Longitudinal analysis of corneal topography in suspected keratoconus. Br. J. Ophthalmol., 93, 815-819.

34 Li, X., Rabinowitz, Y. S., Rasheed, K., Yang, H. (2004). Longitudinal study of the normal eyes in unilateral keratoconus patients. Ophthalmology, 111, 440-446.

35 Ambrosio, R. Jr., Lopes, B. T., Faria-Correia, F., Salomao, M. Q., Buhren, J., Roberts, C. J., Elsheikh, A., Vinciguerra, R., Vinciguerra, P. (2017). Integration of Scheimpflug-Based Corneal Tomography and Biomechanical Assessments for Enhancing Ectasia Detection. J. Refract. Surg., 33, 434-443.

36 Herber, R., Hasanli, A., Lenk, J., Vinciguerra, R., Terai, N., Pillunat, L. E., Raiskup, F. (2022). Evaluation of Corneal Biomechanical Indices in Distinguishing Between Normal, Very Asymmetric, and Bilateral Keratoconic Eyes. J. Refract. Surg., 38, 364-372.

37 Labiris, G., Gatzioufas, Z., Sideroudi, H., Giarmoukakis., A, Kozobolis, V., Seitz, B. (2013). Biomechanical diagnosis of keratoconus: evaluation of the keratoconus match index and the keratoconus match probability. Acta Ophthalmol., 91, e258-262.

38 Fontes, B. M., Ambrósio, R., Jardim, D., Velarde, G. C., Nosé, W. (2010). Corneal biomechanical metrics and anterior segment parameters in mild keratoconus. Ophthalmology, 117, 673–679.

39 Fontes, B. M., Ambrosio, R., Jr., Velarde, G. C., Nose, W. (2011). Ocular response analyzer measurements in keratoconus with normal central corneal thickness compared with matched normal control eyes. J. Refract. Surg., 27, 209-215.

40 Koh, S., Ambrosio, R, Jr., Inoue, R., Maeda, N., Miki, A., Nishida, K. (2019). Detection of Subclinical Corneal Ectasia Using Corneal Tomographic and Biomechanical Assessments in a Japanese Population. J. Refract. Surg., 35, 383-390.

41 Steinberg, J., Siebert, M., Katz, T., Frings, A., Mehlan, J., Druchkiv, V., Buhren, J., Linke, S. J. (2018). Tomographic and Biomechanical Scheimpflug Imaging for Keratoconus Characterization: A Validation of Current Indices. J. Refract. Surg., 34, 840-847.

42 Choi, R. Y., Coyner, A. S., Kalpathy-Cramer, J., Chiang, M. F., Campbell, J. P. (2020). Introduction to Machine Learning, Neural Networks, and Deep Learning. Transl. Vis. Sci. Technol., 9, 14.

43 Koc, M., Aydemir, E., Tekin, K., Inanc, M., Kosekahya, P., Kiziltoprak, H. (2019). Biomechanical Analysis of Subclinical Keratoconus With Normal Topographic, Topometric, and Tomographic Findings. J. Refract. Surg., 35, 247-252.

44 Kataria, P., Padmanabhan, P., Gopalakrishnan, A., Padmanaban, V., Mahadik, S., Ambrósio, R. (2019). Accuracy of Scheimpflug-derived corneal biomechanical and tomographic indices for detecting subclinical and mild keratectasia in a South Asian population. J. Cataract Refract. Surg., 45, 328-336.

45 Ambrosio, R. Jr., Machado, A. P., Leao, E., Lyra, J. M. G., Salomao, M. Q., Esporcatte, L. G. P., Filho, J., Ferreira-Meneses, E., Sena, N. B. Jr., Haddad, J. S., Neto, A. C., Castelo de Almeida, G. Jr., Roberts, C. J., Elsheikh, A., Vinciguerra, R., Vinciguerra, P., Buhren, J., Kohnen, T., Kezirian, G. M., Hafezi, F., Hafezi, N. L., Torres-Netto, E. A., Lu, N., Kang, D. S. Y., Kermani, O., Koh, S., Padmanabhan, P., Taneri, S., Trattler, W., Gualdi, L., Salgado-Borges, J., Faria-Correia, F., Flockerzi, E., Seitz, B., Jhanji, V., Chan, T. C. Y., Baptista, P. M., Reinstein, D. Z., Archer, T. J., Rocha, K. M., Waring, G. O. 4th, Krueger, R. R., Dupps, W. J., Khoramnia, R., Hashemi, H., Asgari, S., Momeni-Moghaddam, H., Zarei-Ghanavati, S., Shetty, R., Khamar, P., Belin, M. W., Lopes, B. (2023). Optimized artificial intelligence for enhanced ectasia detection using Scheimpflug-based corneal tomography and biomechanical data. Am. J. Ophthalmol., 221, 126-142.